

This discussion paper is/has been under review for the journal Atmospheric Chemistry and Physics (ACP). Please refer to the corresponding final paper in ACP if available.

Contribution of garbage burning to chloride and PM_{2.5} in Mexico City

G. Li^{1,2}, W. Lei¹, N. Bei¹, and L. T. Molina^{1,2}

¹Molina Center for the Energy and the Environment, La Jolla, CA, USA

²Massachusetts Institute of Technology, Cambridge, MA, USA

Received: 12 May 2012 – Accepted: 24 May 2012 – Published: 1 June 2012

Correspondence to: G. Li (lgh@mce2.org), L. T. Molina (ltmolina@mit.edu)

Published by Copernicus Publications on behalf of the European Geosciences Union.

13667

Abstract

The contribution of garbage burning (GB) emissions to chloride and PM_{2.5} in the Mexico City Metropolitan Area (MCMA) is investigated for the period of 24 to 29 March during the MILAGRO-2006 campaign using the WRF-CHEM model. When the MCMA-2006 official emission inventory without biomass burning is used in the simulations, the WRF-CHEM model significantly underestimates the observed particulate chloride in the urban and the suburban areas. The inclusion of GB emissions substantially improves the simulations of particulate chloride; GB contributes more than 60 % of the observation, indicating it is a major source of particulate chloride in Mexico City. GB yields up to 3 pbb HCl at the ground level in the city, which is mainly caused by the burning of polyvinyl chloride (PVC) in the garbage. GB is also an important source of PM_{2.5}, contributing about 3–30 % simulated PM_{2.5} mass on average. More modeling work is needed to evaluate the GB contribution to hazardous air toxics, such as dioxin, which is found to be released at high level from PVC burning in laboratory experiments.

1 Introduction

Biomass burning (BB) is an important source of ambient PM_{2.5} (particulate matter with aerodynamic diameter less than 2.5 μm) and emits approximately more than 80 % of total carbonaceous aerosol mass in the atmosphere (Andreae and Merlet, 2001; Bond et al., 2004). BB aerosols not only adversely affect human health and air quality from regional to global scales (Lighty et al., 2000; Lelieveld et al., 2001), but also contribute to the large uncertainty in the current understanding of radiative forcing (IPCC, 2007). Depending on the nature of the burned biomass and the burning conditions, BB aerosols have varying capacities for absorbing and reflecting incident solar radiation, with a direct radiative forcing of $+0.03 \pm 0.12 \text{ W m}^{-2}$ globally (IPCC, 2007). Considering micro-physical interactions between aged BB aerosols and clouds (aerosol indirect effect), an

13668

even greater uncertainty is involved when trying to determine the BB aerosol climate forcing (Brioude et al., 2009; Randles and Ramaswamy, 2010; Grell et al., 2011).

Wild fires and combustion of biofuel are the two largest types of global BB. Recent field measurements in central Mexico by Christian et al. (2010) have shown that garbage burning (GB) may be a commonly overlooked important global source of emissions, considering the global garbage generation of about 2000 Tg yr^{-1} with half burned.

Open garbage burning is a common practice to dispose of solid waste that takes place in both developing and developed countries. In developed countries, this practice mainly takes place in rural areas where collection of municipal waste is not as efficient as in urban areas and is usually done in the backyard of houses. For example, in rural areas of the US, about 12–40% of households burn garbage in their backyards (US EPA, 2006). In developing countries, open garbage burning occurs in locations where collection and management of solid waste are not implemented or inadequate, even in urban areas, and includes backyard burning and open dump burning. Open garbage burning produces smoke and emits a wide variety of compounds including black carbon, air toxics and Greenhouse gases (Costner, 2005, 2006). In addition to the release of toxic chemicals that are harmful to human health, the smoke from the fire can deposit chemicals on garden vegetables, crops and soil and eventually entering into the food chain.

Christian et al. (2010) estimated a fine particle emission factor for GB in Central Mexico of about 10.5 g kg^{-1} and observed large HCl emission factor in the range of $2\text{--}10 \text{ g kg}^{-1}$. They also suggested that GB is a major source of HCl and may generate as much as $6\text{--}9 \text{ Tg yr}^{-1}$ globally. Numerous studies have attempted to evaluate the impact of BB from wild fires on local and regional air quality using chemical transport models (e.g., Wang and Christopher, 2006; Zeng et al., 2008; Tian et al., 2009). Previous studies have shown that the air quality in Mexico City is frequently influenced by open biomass burning from nearby mountains and savannas surrounding the city (Molina et al., 2010). However, few studies have been conducted to investigate the impact of

13669

GB on air quality due to lack of the observed emission factor and emission estimates of trace gases and particles for GB. During the MCMA-2006 field campaign as part of the MILAGRO (Megacity Initiative: Local and Global Research Observations) project conducted in March 2006, an extensive data set relevant to emissions, transport and transformations of pollutants was obtained, including highly time-resolved ambient gas phase species and aerosols (Molina et al., 2010). In addition, during the spring of 2007, Christian et al. (2010) and Yokelson et al. (2011) measured the initial emissions of trace gases and aerosol speciation for elemental and organic carbon (EC and OC), anhydrosugars, Cl^{-1} , NO_3^{-1} , and 20 metals from several garbage fires in Central Mexico and obtained the emission factors of trace gases and particles for GB. All of these observations have provided an opportunity to assess the contribution of GB to the air quality in a polluted urban area.

The purpose of this study is to evaluate the impacts of GB on the air quality, particularly the contribution of GB on chloride and $\text{PM}_{2.5}$, for Mexico City using the WRF-CHEM model based on the measurements taken during MCMA-2006. The WRF-CHEM model and the model configuration are described in Sect. 2. Results of the modeling experiments and comparisons are presented in Sect. 3, and the Conclusions are given in Sect. 4.

2 Model and method

2.1 WRF-CHEM model

The WRF-CHEM model used in the present study is developed by Li et al. (2010, 2011b, c) at Molina Center for Energy and the Environment, with a new flexible gas phase chemical module which can be utilized in different chemical mechanisms, including CBIV, RADM2, and SAPRC. The gas-phase chemistry is solved by an Eulerian backward Gauss-Seidel iterative technique with a number of iterations. The short-lived species, such as OH and $\text{O}(^1\text{D})$, are assumed to be in the steady state. The solution

13670

is iterated until all species are within 0.1 % of their previous iterative values. For the aerosol simulations, the CMAQ (version 4.6) aerosol module developed by EPA, which is designed to be an efficient and economical depiction of aerosol dynamics in the atmosphere, is incorporated in the WRF-CHEM model (Binkowski and Roselle, 2003). In this aerosol component, the particle size distribution is represented as the superposition of three lognormal sub-distributions, called modes. The processes of coagulation, particle growth by the addition of mass, and new particle formation are included. The wet deposition also follows the method used in the CMAQ/Models3. Surface deposition of chemical species is parameterized following Wesely (1989). The photolysis rates are calculated using the FTUV (Tie et al., 2003; Li et al., 2005).

The inorganic aerosols are predicted in the WRF-CHEM model using ISORROPIA Version 1.7 (<http://nenes.eas.gatech.edu/ISORROPIA/>), which calculates the composition and phase state of an ammonium-sulfate-nitrate-chloride-sodium-calcium-potassium-magnesium-water inorganic aerosol in thermodynamic equilibrium with gas phase precursors. The kind of thermodynamic equilibrium is delicately dependent on the environmental humidity and temperature. In this study, ISORROPIA is mainly utilized to predict the thermodynamic equilibrium between the ammonia-sulfate-nitrate-chloride-water aerosols and their gas phase precursors of H_2SO_4 - HNO_3 - NH_3 - HCl -water vapor.

The secondary organic aerosol (SOA) formation is simulated using a non-traditional SOA model including the volatility basis-set modeling method in which primary organic components are assumed to be semi-volatile and photochemically reactive and are distributed in logarithmically spaced volatility bins (Li et al., 2011a). The partitioning of semi-volatile organic species is calculated using the algorithm suggested by Koo et al. (2003), in which the bulk gas and particle phases are in equilibrium and all condensable organics form a pseudo-ideal solution (Odum et al., 1996). Nine surrogate species with saturation concentrations from 10^{-2} to $10^6 \mu\text{g m}^{-3}$ at room temperature are used for the primary organic aerosol (POA) components following the approach of

13671

Shrivastava et al. (2008). Detailed description about the volatility basis-set approach can be found in Li et al. (2011a).

2.2 Model configuration

Two three-day episodes are selected in the present study: (1) 24–26 March 2006, and (2) 27–29 March 2006, representing typical “ O_3 -Convection South” and “ O_3 -Convection North” meteorological conditions in Mexico City, respectively (de Foy et al., 2008), with minor impacts of wildfire BB. O_3 -Convection South takes place when there is a weak northerly wind component aloft with rain in the southern part of the Mexico City basin. O_3 -Convection North occurs when there is a weak southerly wind component aloft with a gap flow and rain in the northern part of the basin. The WRF-CHEM model is configured with one grid with spacing of 3 km (99×99 grid points) centered at 19.538°N and 99°E (Fig. 1). Thirty-five vertical levels are used in a stretched vertical grid with spacing ranging from 50 m near the surface, to 500 m at 2.5 km and 1 km above 14 km altitude. The model employs the Lin microphysics scheme (Lin et al., 1983), the Yonsei University (YSU) PBL scheme (Noh et al., 2001), the Noah land-surface model (Chen and Dudhia, 2000), the longwave radiation parameterization (Mlawer et al., 1997), and the shortwave radiation parameterization (Dudhia, 1989). The meteorological initial and boundary conditions are from NCEP $1 \times 1^\circ$ reanalysis data. The chemical initial and boundary conditions are interpolated from MOZART 3-hour output (Horowitz et al., 2003).

The non-BB emission inventory (EI) used in the present study is the 2006 EI developed at Molina Center with the primary PM emissions (Song et al., 2010). The POA emissions are redistributed following the study of Tsimpidi et al. (2010). The GB EI was developed based on the garbage fire emissions factors measured during MILAGRO (Christian et al., 2010) and the literature (Lemieux et al., 2004; Akagi et al., 2011), in conjunction with a 1×1 km spatial distribution of population and socioeconomic classifications in Mexico City (Hodzic et al., 2012). The uncertainty of the estimated GB emissions is a factor of 2 or more. This GB emission inventory has recently been ap-

13672

plied in two model-based studies to investigate the GB impacts on air quality in Mexico City (Hodzic et al., 2012; Lei et al., 2012). In order to evaluate the GB contributions to chloride, the measured emission factors of particulate chloride and HCl by Christian et al. (2010) are used in this study: 0.467 g particulate chloride and 4.82 g HCl per kg fuel burned, respectively.

Two case simulations are performed in this study. In the first case, only the non-BB emissions are considered in simulations (hereafter referred to as B-case). In the second case (hereafter referred to as G-case), the GB emissions are included together with the non-BB emissions. We compare the model results from the B-case and G-case with measurements obtained at the T0 urban supersite and T1 suburban supersite, and evaluate the GB contributions to chloride and $PM_{2.5}$.

3 Results

The WRF-CHEM model performance during the simulation period from 24 to 29 March 2006 in Mexico City can be found in Li et al. (2011a, b). In general, the WRF-CHEM model performs well in modeling the temporal variations and spatial distributions of O_3 and CO compared with the measurements at RAMA (ambient air monitoring network) sites during daytime, but the simulated nighttime O_3 and CO deviate frequently from the observation due to the difficulties in modeling the meteorological fields at nighttime and the complexity of the nighttime chemistry (Li et al., 2011a). In addition, the simulated organic, black carbon, nitrate, and ammonium aerosols are in good agreement with the surface observations at T0 and aircraft measurements. The WRF-CHEM has difficulties in simulating sulfate aerosols, which are influenced by multiple sources with substantial emission uncertainties in Mexico City (Li et al., 2011b).

Figure 2a shows the diurnal profiles of simulated and observed particulate chloride at T0 from 24 to 29 March, 2006. The particulate chloride at T0 was measured using a High-Resolution Time-of-Flight Aerosol Mass Spectrometer (HR-ToF-AMS) and complementary instrumentation during MILAGRO field campaign (Aiken et al., 2009). The

13673

observed particulate chloride shows large late night/early morning spikes, especially in the early morning on 25, 26 and 29 March, with mass concentrations exceeding $3 \mu g m^{-3}$. In the B-case with only non-BB emissions, the particulate chloride concentrations are underestimated substantially compared to the observations, particularly during early morning. When the GB emissions are considered in the G-case, the WRF-CHEM model tracks reasonably well the particulate chloride diurnal variability compared with the measurement at T0. For example, the occurrence of peak particulate chloride concentrations is well replicated, and the accumulation of nighttime particulate chloride concentrations and the rapid falloff of late morning particulate chloride concentrations are also reproduced. However, the G-case frequently underestimates the observed particulate chloride spikes, especially in the early morning on 25 and 26 March, indicating either unawareness of unknown sources or uncertainties from meteorological field simulations. Figure 2b shows the diurnal cycle of observed and simulated particulate chloride concentrations at T0 over the simulation period. Both the B-case and G-case show good performance in simulating the particulate chloride diurnal cycles, but the B-case underestimates the observed particulate chloride during the entire daily cycle, producing about less than 40% of the observations. The modeled particulate chloride concentrations in the G-case are more consistent with the observations than those from the B-case, with a mean concentration of $0.41 \mu g m^{-3}$, very close to the observed $0.42 \mu g m^{-3}$. Compared the simulated chloride in the B-case and G-case, GB contributes about $0.24 \mu g m^{-3}$ chloride mass on average, or 60% of the observation at T0, demonstrating that GB is a dominant source of particulate chloride in the urban area.

T1 is a supersite located in the northwestern part of the Mexico City basin and used as a suburban background site during MILAGRO field campaign (Molina et al., 2010). The simulated particulate chloride is compared to the particle-into-liquid-sampler (PILS) measurement at T1 (Fig. 2c and d). The measured particulate chloride exhibits distinct peaks during midnight and early morning. The B-case very severely underestimates the observed particulate chloride concentrations during the entire sim-

13674

ulation period, suggesting that the contribution of the non-BB emissions to the particulate chloride is negligible in the suburban area. GB emissions considerably improve the particulate chloride simulations in the G-case, and the WRF-CHEM model generally captures the peaks during early morning, but overestimates on 27 March and underestimates on 28 and 29 March. Although the G-case includes the GB emissions, it still fails to produce the high peak between 00:00 and 02:00 LT (Fig. 2d), which is possibly caused by other particulate chloride sources, such as agricultural fires, brick making kilns and volcanoes, that are not yet considered in the present study. Due to frequent absence of observed particulate chloride at T1 in the afternoon, only the comparison of mean particulate chloride mass in the morning is made between model and measurement. The simulated mean chloride mass from GB in the morning is about $0.26 \mu\text{g m}^{-3}$, which is 62 % of the observed value ($0.42 \mu\text{g m}^{-3}$), showing that GB is a major source of particulate chloride in the suburban area.

Christian et al. (2010) measured high HCl emission factor from GB in Mexico, suggesting that GB is an important source of HCl. Figure 3 illustrates the modeled six-day averaged ground level distributions of HCl from GB at 09:00 LT (local time) and 15:00 LT. At 09:00 LT, due to the weak winds and low planetary boundary layer (PBL) height, which are favorable for the accumulation of HCl, high levels of HCl, up to 1 ~ 3 ppb, are predicted near the GB emission source, and the HCl concentrations in most of Mexico City exceed 0.5 ppb. At 15:00 LT, with the transport and mixing of smoke plumes and increase of PBL height, the simulated surface HCl concentrations decrease to 0.1 ~ 1.0 ppb in Mexico City. Based on the measurement of an open-path Fourier Transform Infrared (FTIR), Moya et al. (2003) estimated that the HCl concentration did not exceed 2–3 ppb level in Mexico City. In addition, San Martini et al. (2006) suggested that the most likely concentrations of HCl are in the sub-ppb range in Mexico City when the particles are aqueous from the simulations of a Markov Chain Monte Carlo model with a thermodynamic equilibrium model during the MCMA-2003 campaign (Molina et al., 2007). The WRF-CHEM simulations of HCl from GB are compa-

13675

nable to the above two studies, showing that GB is a major source of HCl in Mexico City.

Li et al. (2011a) have simulated organic aerosol concentrations using the WRF-CHEM model in Mexico City during the same period as this study, and found that, with the contribution of glyoxal and methylglyoxal, the non-traditional SOA model can explain over 80 % observed SOA in the urban area, but the contributions of BB to organic aerosols are not considered in Li et al. (2011a). In the present study, the six-day episode we have chosen has been reported to have minor impacts from wild fire burning (Aiken et al., 2009; Lei et al., 2012), and the GB emissions could constitute an important source of biomass burning organic aerosols (BBOA). Figure 4a presents the diurnal profiles of simulated (POA in the G-case minus POA in the B-case) and observed BBOA at T0. Although the WRF-CHEM model fails to capture the large fluctuations of the observed BBOA concentrations, in general it reproduces the observed diurnal cycle (Fig. 4b). The simulated six-day averaged BBOA mass is close to the measurement at T0, demonstrating that GB is a major source of BBOA in the urban area when wild fires around Mexico City are sparse. The WRF-CHEM model generally underestimates the observed BBOA at T1 (Fig. 4c and d) and produces more than 50 % of the observations, indicating that other biofuel emissions, such as domestic (food cooking) and industrial biofuel use, could also play an important role in BBOA concentrations in the suburban area. SOA formation due to the GB emissions also improves the SOA simulations at T0 and T1 during daytime (Fig. 4e and f). GB can explain 10 % and 18 % observed SOA concentrations on average at T0 and T1, respectively. The SOA contribution due to GB emissions enhances the domain-wide organic aerosol by about 4.4 % on average, which is close to the results by Lei et al. (2012). Lei et al. (2012) estimated that the SOA from GB contributes about 5 % to organic aerosols in both the urban and suburban areas of the MCMA. Detailed evaluation of GB emissions to organic aerosols (OA) can be found in Lei et al. (2012).

Figure 5a shows the diurnal profiles of simulated and observed near-surface $\text{PM}_{2.5}$ concentrations averaged over Mexico City RAMA stations and T1. The WRF-CHEM

13676

model generally tracks the temporal variations of $PM_{2.5}$ concentrations reasonably well, but frequently underestimates during daytime, particularly between 09:00 and 11:00 LT in the morning when the observed $PM_{2.5}$ concentrations reach peaks due to the accumulation of primary aerosols and efficient formation of secondary aerosols under condition of relatively low PBL height. The nighttime simulated $PM_{2.5}$ concentrations are higher than the observations (Fig. 4b), irregardless of whether the GB emissions are included or not, indicating either the failure of PBL simulations or inefficiency of the pollutant dispersion process or problems with the emissions during nighttime (Li et al., 2011a). However, during daytime, GB emissions considerably improve the $PM_{2.5}$ simulations. On average, the B-case yields $23.1 \mu\text{g m}^{-3}$ $PM_{2.5}$ averaged over the RAMA sites and T1, lower than the observed $25.8 \mu\text{g m}^{-3}$. GB emissions in the G-case enhance the $PM_{2.5}$ mass by about 13 % or $3.0 \mu\text{g m}^{-3}$ compared to the B-case. In addition, GB emissions contribute about 3–30 % of simulated $PM_{2.5}$ in Mexico City at 09:00 and 15:00 LT (Fig. 4c and d), which is consistent with the conclusion reported by Christian et al. (2010) from the measurement of fine particle antimony (Sb) from GB. They compared the measured mean mass ratios of Sb/ $PM_{2.5}$ for pure garbage burning and ambient air and concluded that GB could account for up to one third of the $PM_{2.5}$ mass in MCMA. On average, GB emissions contribute $1.9 \mu\text{g m}^{-3}$ or 12 % to the $PM_{2.5}$ mass in Mexico City (see the black box in Fig. 5c) in the G-case. About 65 % of the enhanced $PM_{2.5}$ mass from GB is contributed by OA, in which the contributions from POA and SOA are 30 % and 35 %, respectively. The particulate chloride constitutes 10 % of the enhancement of $PM_{2.5}$ mass from GB, greater than the contributions from black carbon (4 %), sulfate (0 %), nitrate (0.8 %), and ammonium (5 %) aerosols. Other unidentified particulate species contributes about 14 % of the GB $PM_{2.5}$ mass. Using the same GB emission inventory as the present study, Hodzic et al. (2012) reported that GB represents 1–15 % of the $PM_{2.5}$ mass over the metropolitan area of Mexico City with strong spatial variability; their estimate is lower than the results from the present study. There are two main reasons for the difference between the two studies. Firstly, in Hodzic et al. (2012), POA is considered physically and chemically inert, resulting in negligible

13677

SOA contribution from GB. In our study, POA is assumed to be semi-volatile and photochemically reactive; GB considerably enhances the SOA formation in Mexico City. Secondly, Hodzic et al. (2012) did not consider the contribution of chloride to the $PM_{2.5}$ mass, which is not negligible according to our estimation. If the contribution of SOA and chloride from GB are excluded, the results in this present study are comparable to those in Hodzic et al. (2012).

4 Summary and implication

In the present study, the WRF-CHEM model has been used to evaluate the contributions of GB to chloride and $PM_{2.5}$ in Mexico City during the period from 24 to 29 March 2006. Based on the recently developed GB emission inventory (Hodzic et al., 2012; Lei et al., 2012), the simulated particulate chloride from GB can explain over 60 % of the observation in the urban and suburban area, indicating that GB is a major source of particulate chloride in Mexico City. In addition, GB also contributes up to 3 ppb HCl, which is consistent with the measurement in Mexico City. GB is also an important source of $PM_{2.5}$, constituting about 3–30 % simulated $PM_{2.5}$ mass on average. It should be emphasized that the GB emission inventory used in the present study still has large uncertainties, which potentially influence the evaluation of the contribution of GB to chloride and $PM_{2.5}$ in Mexico City. Although the simulated $PM_{2.5}$ from GB is consistent with the measurement by Christian et al. (2010), showing the present GB emission inventory is generally reasonable, the uncertainties of GB emissions need to be further investigated to provide a bolster for the model simulations. Furthermore, it is worthy to note that meteorological conditions play a key role in determining the accumulation or dispersion of pollutant and might significantly influence the evaluation of the GB contribution to chloride and $PM_{2.5}$ (Bei et al., 2008, 2010).

Christian et al. (2010) suggested that large HCl emission factor in central Mexico results from the burning of polyvinyl chloride (PVC). A recent study by Hedman et al. (2006) showed that chloride-containing plastic waste gave rise to high emis-

13678

- Noh, Y., Cheon, W. G., and Raasch, S.: The improvement of the K-profile model for the PBL using LES. Preprints, Int. Workshop of Next Generation NWP Models, Seoul, South Korea, Laboratory for Atmospheric Modeling Research, 65–66, 2001.
- 5 Odum, J. R., Hoffman, T., Bowman, F., Collins, D., Flagan, R. C., and Seinfeld, J. H.: Gas/particle partitioning and secondary organic aerosol yields, *Environ. Sci. Technol.*, 30, 2580–2585, 1996.
- 10 Randles, C. A. and Ramaswamy, V.: Direct and semi-direct impacts of absorbing biomass burning aerosol on the climate of southern Africa: a Geophysical Fluid Dynamics Laboratory GCM sensitivity study, *Atmos. Chem. Phys.*, 10, 9819–9831, doi:10.5194/acp-10-9819-2010, 2010.
- 15 San Martini, F. M., Dunlea, E. J., Volkamer, R., Onasch, T. B., Jayne, J. T., Canagaratna, M. R., Worsnop, D. R., Kolb, C. E., Shorter, J. H., Herndon, S. C., Zahniser, M. S., Salcedo, D., Dzepina, K., Jimenez, J. L., Ortega, J. M., Johnson, K. S., McRae, G. J., Molina, L. T., and Molina, M. J.: Implementation of a Markov Chain Monte Carlo method to inorganic aerosol modeling of observations from the MCMA-2003 campaign – Part II: Model application to the CENICA, Pedregal and Santa Ana sites, *Atmos. Chem. Phys.*, 6, 4889–4904, doi:10.5194/acp-6-4889-2006, 2006.
- 20 Shrivastava, M. K., Lane, T. E., Donahue, N. M., Pandis, S. N., and Robinson, A. L.: Effects of gas-particle partitioning and aging of primary emissions on urban and regional organic aerosol concentrations, *J. Geophys. Res.*, 113, D18301, doi:10.1029/2007JD009735, 2008.
- Song, J., Lei, W., Bei, N., Zavala, M., de Foy, B., Volkamer, R., Cardenas, B., Zheng, J., Zhang, R., and Molina, L. T.: Ozone response to emission changes: a modeling study during the MCMA-2006/MILAGRO Campaign, *Atmos. Chem. Phys.*, 10, 3827–3846, doi:10.5194/acp-10-3827-2010, 2010.
- 25 Tian, D., Hu, Y. T., Wang, Y. H., Boylan, J. W., Zheng, M., and Russell, A. G.: Assessment of biomass burning emissions and their impacts on urban and regional $PM_{2.5}$: A Georgia case study, *Environ. Sci. Technol.*, 43, 299–305, 2009.
- Tie, X., Madronich, S., Walters, S., Zhang, R., Rasch, P., and Collins, W.: Effect of clouds on photolysis and oxidants in the troposphere, *J. Geophys. Res.*, 108, 4642, doi:10.1029/2003JD003659, 2003.
- 30 Tsimpidi, A. P., Karydis, V. A., Zavala, M., Lei, W., Molina, L., Ulbrich, I. M., Jimenez, J. L., and Pandis, S. N.: Evaluation of the volatility basis-set approach for the simulation of organic

13683

- aerosol formation in the Mexico City metropolitan area, *Atmos. Chem. Phys.*, 10, 525–546, doi:10.5194/acp-10-525-2010, 2010.
- 5 USEPA: An inventory of sources and environmental releases of dioxin-like compounds in the United States for the years 1987, 1995, and 2000, EPA/600/P-03/002F, National Center for Environmental Assessment, Office of Research and Development, Washington, DC, 677 pp., 2006.
- 10 Wang, J. and Christopher, S. A.: Mesoscale modeling of central American smoke transport to the United States, 2: Smoke regional radiative impacts on surface energy budget and boundary layer evolution, *J. Geophys. Res.*, 111, D14S92, doi:10.1029/2005JD006720, 2006.
- Wesely, M. L.: Parameterization of surface resistance to gaseous dry deposition in regional-scale numerical models, *Atmos. Environ.*, 23, 1293–1304, 1989.
- 15 Yokelson, R. J., Burling, I. R., Urbanski, S. P., Atlas, E. L., Adachi, K., Buseck, P. R., Wiedinmyer, C., Akagi, S. K., Toohey, D. W., and Wold, C. E.: Trace gas and particle emissions from open biomass burning in Mexico, *Atmos. Chem. Phys.*, 11, 6787–6808, doi:10.5194/acp-11-6787-2011, 2011.
- Zeng, T., Wang, Y. H., Yoshida, Y., Tian, D., Russell, A. G., and Barnard, W. R.: Impacts of prescribed fires on air quality over the southeastern United States in spring based on modeling and ground/satellite measurements, *Environ. Sci. Technol.*, 42, 8401–8406, 2008.

13684

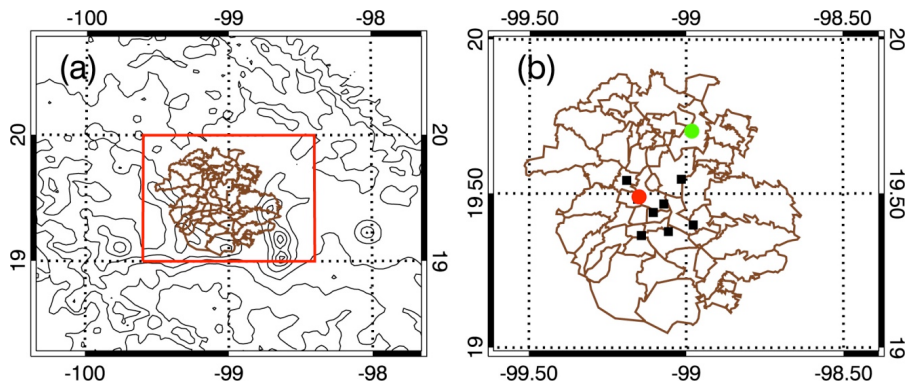


Fig. 1. WRF-CHEM simulation domain. Black squares represent the RAMA (Mexico City Ambient Air Monitoring Network) sites with $PM_{2.5}$ measurements. The red and green circles represent the T0 and T1 supersites, respectively.

13685

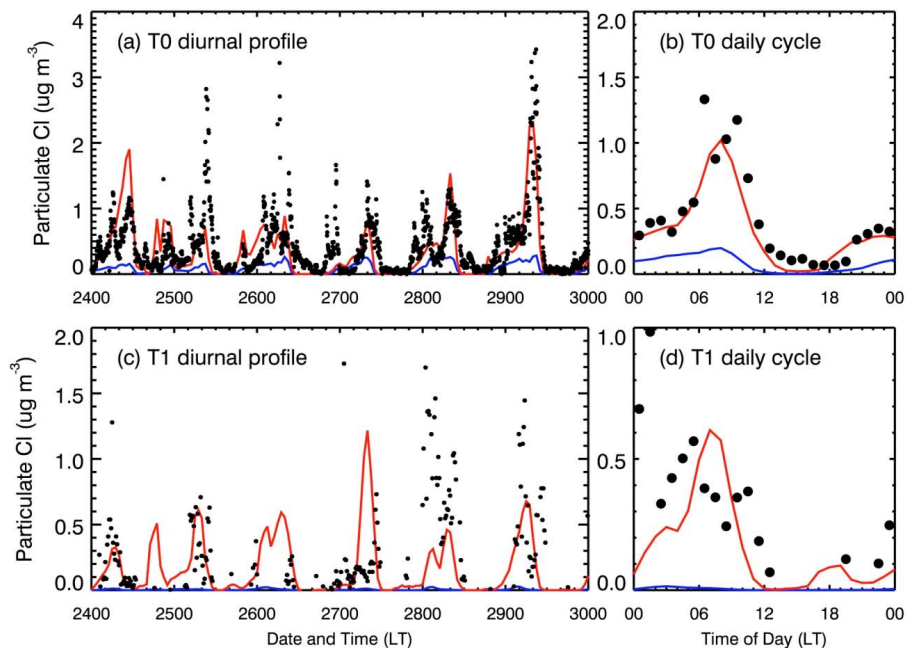


Fig. 2. Diurnal profiles of measured and simulated particulate chloride concentrations at (a) T0 and (c) T1 during the period from 24 to 29 March 2006, and diurnal cycles of measured and simulated particulate chloride concentrations at (b) T0 and (d) T1 averaged during the simulation period. Black dots: measurements; red line: the G-case with GB emissions; Blue line: the B-case without GB emissions.

13686

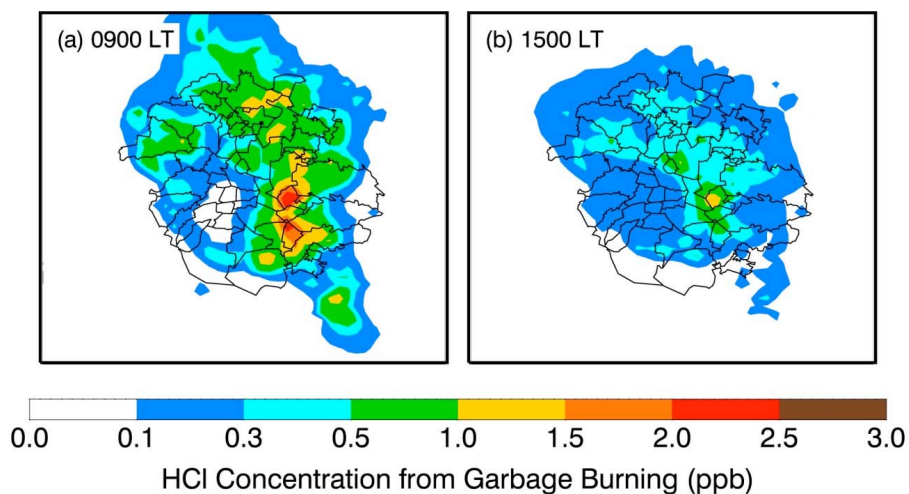


Fig. 3. Simulated HCl distributions from GB at (a) 09:00 and (b) 15:00 LT over Mexico City averaged during the period from 24 to 29 March 2006.

13687

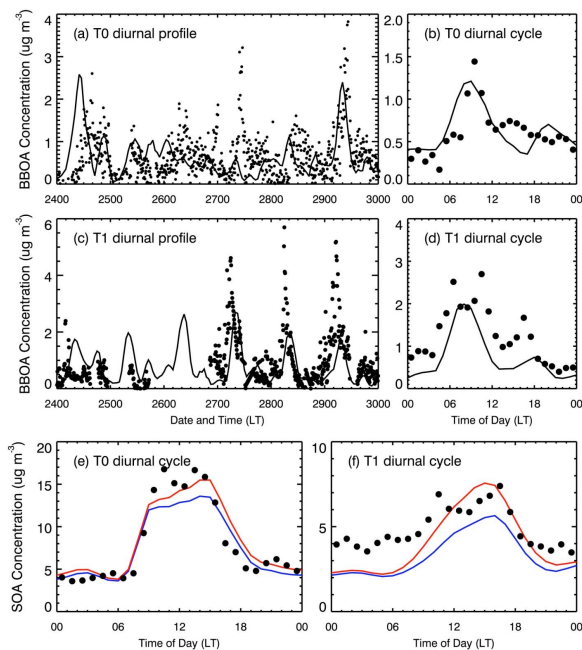


Fig. 4. Diurnal profiles of measured and simulated BBOA concentrations at (a) T0 and (c) T1 during the period from 24 to 29 March 2006. Diurnal cycles of measured and simulated BBOA concentrations at (b) T0 and (d) T1, and SOA concentrations at (e) T0 and (f) T1 averaged during the simulation period. Black dots: measurements; black line: simulated BBOA (POA in G-case minus POA in B-case); red line: the G-case with GB emissions; Blue line: the B-case without GB emissions.

13688

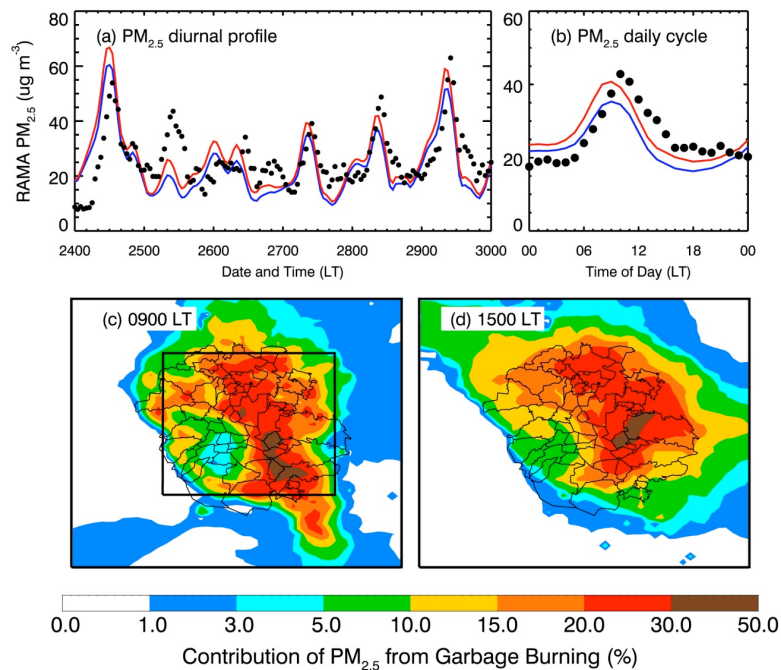


Fig. 5. (a) diurnal profile of measured and simulated PM_{2.5} concentrations from GB averaged over RAMA sites and during the period from 24 to 29 March 2006; (b) diurnal cycles of measured and simulated PM_{2.5} concentrations from GB averaged over RAMA sites and during the simulation period; GB Contribution to PM_{2.5} concentrations at (c) 09:00 and (d) 15:00 LT over Mexico City averaged during the simulation period. Black dots: measurements; red line: the G-case with GB emissions; Blue line: the B-case without GB emissions.